Indian Journal of Chemistry
Vol. 60A, September 2021, pp. 1181-1191

Molecular structure, spectroscopic and DFT studies of 2-(4 ethoxyphenyl) isoindoline-1,3-dione

Meryem Evecen[a,*], Hasan Tanak[a], Gülcan Duru[a], Seher Meral[b] & Ayşen Alaman Ağar[c]

[a]Department of Physics, Faculty of Arts and Sciences, Amasya University, 05100, Amasya, Turkey

[b]Boyabat Vocational School, Sinop University, Sinop, Turkey

[c]Department of Chemistry, Faculty of Arts and Sciences, Ondokuz Mayıs University, 55139, Samsun, Turkey

*E-mail: meryem.evecen@amasya.edu.tr

Received 21 October 2020; revised and accepted 06 August 2021

2-(4-Ethoxyphenyl)isoindoline-1,3-dione molecule has been characterized by experimental FT-IR and UV-visible spectroscopic methods. Density fuctional theory calculations of the molecular structure and vibrational spectra have been performed using the B3LYP/6-311++G(d,p) level of theory for the 2-(4-ethoxyphenyl)isoindoline-1,3-dione. The theoretical results are compared with the experimental observations. Using the TD-DFT methodology, the electronic absorption spectra of the investigated molecule have been calculated. The enthalpy, entropy and heat capacity properties based on the vibrational calculations are calculated at different temperatures. Besides, the frontier orbitals, atomic charges, reactivity descriptors, molecular electrostatic potential, interaction energies and nonlinear optical properties are predicted by the density functional theory calculations.

Keywords: Isoindoline, DFT, TD-DFT, Vibrational calculations, Nonlinear optical properties, Reactivity descriptors

Scientists have been fascinated for decades by isoindoline and its derivatives which is also found in a number of natural and pharmaceutical compounds[1,2]. The structural features of isoindole-1,3-dione conferred biological activity and pharmaceutical use[3-5], so used as a precursor compound. The phthalimido moiety, also known as pharmacophore, has large-scale activities such as anticonvulsant[6], anxiogenic[7], antitumor[8,9], antihyperlipidemic and anti-inflammatory activities[10-14]. They also contain many biologically active compounds and drugs as structure fragments[15-19]. Unexpectedly, in the 1950s, a drug based phthalimide used by pregnant women caused numerous birth defects[20]. Some of isoindole-1,3-dione have been also used as an intermediate in chemical production such as in pharmacy, medicine, pesticides, dyes, etc.[21]. In addition, some have been used in halogenation reactions[22]. It has also benefitted the imide derivatives in the reactions involving cyclocondensation, acylation and alkylation[23,24]. The compounds also carry industrial importance. For instance, they also act like bleaching detergents, heat resistant polymers and antidepressants. In addition they are also used in chemical synthesis and in plastics[25].

Density functional theory (DFT) methods are very popular in molecular computations. The calculation of many molecular properties became probable with developing the exchange-correlation functionals. In literature, it was presented that DFT displays a high accuracy with experimental results for molecular geometry, electronic transition, frequency, etc.[26-28].

In previous work, 2-(4-ethoxyphenyl)isoindoline-1,3-dione (EPID) was synthesized and characterized by X-ray diffraction study[29]. Despite the above-mentioned importance of EPID, its theoretical calculations, especially spectroscopic properties, have not been investigated so far. In this work, DFT/ B3LYP method has been used to calculate molecular structure and vibrational wavenumbers of EPID. The electronic absorption spectra, reactivity descriptors, molecular electrostatic potential (MEP), nonlinear optical properties (NLO), natural bond orbitals (NBO) and thermodynamical functions of the compound have been predicted theoretically. Comparisons between calculations and experiments are also made.

Materials and Methods

Measurements

Infrared (IR) spectra were measured in Schmadzu FTIR-8900 spectrophotometer in the range 4000-400 cm^{-1}. The UV–visible spectroscopy measurements were assessed on a Unicam UV-visible spectrophotometer in EtOH.

Theoretical methods

Theoretical computations were performed by using Gaussian 09W program[30]. The optimized geometry and vibrational wavenumber calculations of EPID molecule were performed by DFT/B3LYP method with the 6-311++G(d,p) basis set. The theoretical wavenumbers were scaled by 0.96 for the optimized structure. The molecular structure and vibrational motions were visualized by GaussView 5 program[31]. The entropy, enthalpy and heat capacity properties of the compound were predicted based on the vibrational analysis at different temperatures. The theoretical electronic absorption spectra studies were performed by aid of the TD-DFT methodology[32] in gas phase. The solvent effect on the electronic absorption spectra has been taken into consideration by using the integral equation formalism polarisable continuum model (IEF-PCM)[33]. Ethanol was used as solvent. The atomic charges of EPID were investigated by DFT calculations in two solvents (ε=78.39, water; ε=24.55, ethanol) at the B3LYP/6-311++G(d,p) level using the IEF-PCM method. The frontier molecular orbital, NLO, MEP and NBO calculations were also predicted using the DFT/B3LYP method.

Results and Discussion

Optimized geometry

The ground state optimized geometry and the experimental geometry of EPID are shown in Fig. 1. The most important optimized geometry parameters of EPID have been listed in Table 1. The X-ray structure of EPID is also compared with the optimized

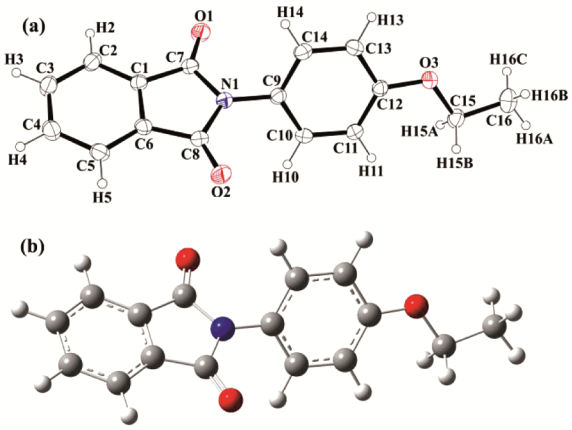

Fig. 1 — (a) Ortep-3 diagram of EPID[29], displacement ellipsoids are drawn at the 30% probability level and H atoms are shown as small spheres of arbitrary radii and (b) The theoretical geometric structure of EPID (with B3LYP/6-311++G(d,p) level)

Table 1 — Selected molecular structure parameters

Parameter	Expt.[29]/ Calc.	Parameters	Exp.[29]/ Cal.
Bond length (Å)		Bond angle (º)	
O3-C12	1.3666 (18)/ 1.362	C12-O3-C15	117.75 (12)/ 119.120
O3-C15	1.4318 (19)/ 1.431	C7-N1-C8	123.75 (12)/ 124.228
O1-C7	1.2074 (19)/ 1.206	C7-N1-C9	124.79 (12)/ 124.317
N1-C7	1.4021 (19)/ 1.415	C14-C9-N1	120.10 (13)/ 120.127
N1-C8	1.4054 (19)/ 1.415	O1-C7-N1	125.45 (14)/ 125.837
N1-C9	1.4351 (19)/ 1.429	O1-C7-C1	128.47 (14)/ 128.416
C9-C14	1.378 (2)/ 1.399	N1-C7-C1	106.07 (12)/ 105.746
C9-C10	1.381 (2)/ 1.391	O3-C12-C11	125.21 (14)/ 124.659
O2-C8	1.2029 (19)/ 1.206	C2-C1-C7	130.35 (15)/ 129.912
C7-C1	1.482 (2)/ 1.491	C6-C1-C7	121.24 (15)/ 121.562
C12-C11	1.380 (2)/ 1.398	O3-C15-C16	107.51 (15)/ 107.682
C12-C13	1.394 (2)/ 1.401	O2-C8-N1	125.13 (15)/ 125.869
C11-C10	1.385 (2)/ 1.395	O2-C8-C6	105.74 (12)/ 105.738
C1-C2	1.384 (2)/ 1.392	N1-C8-C6	129.13 (15)/ 128.393
C1-C6	1.378 (2)/ 1.386	Torsion angle (º)	
C14-C13	1.380 (2)/ 1.385	C7-N1-C9-C14	55.9 (2)/ 49.462
C15-C16	1.504 (3)/ 1.517	C7-N1-C9-C10	-124.53 (16)/ -130.741
C5-C6	1.388 (2)/ 1.399	C8-N1-C9-C10	57.7 (2)/ 49.516
C5-C4	1.382 (2)/ 1.386	C8-N1-C7-O1	-178.25 (16)/ -179.934
C8-C6	1.488 (2)/ 1.491	C15-O3-C12-C11	2.4 (2)/ -0.107
C4-C3	1.376 (3)/ 1.399	C15-O3-C12-C13	-177.42 (15)/ 179.871
C3-C2	1.390 (3)/ 1.399	C12-O3-C15-C16	-179.93 (15)/ 179.622

geometric structure. Some geometrical discrepancies are observed between them (see Fig. 1). The C7-N1-C9-C14, C7-N1-C9-C10 and C8-N1-C9-C10 torsion angles are 55.9°, -124.53°, 57.7°, respectively, for X-ray crystal structure[29]. These torsion angles are calculated as 49.5°, -130.7° and 49.5°, respectively, at B3LYP/6-311++G(d,p) level. Also, the C15-O3-C12-C11, C15-O3-C12-C13 and C12-O3-C15-C16 torsion angles were predicted to be 2.4°, -177.42° and -179.93 ° for X-ray crystal structure[29]. The calculated values are -0.1°, 179.9° and 179.6°, respectively, at B3LYP/6-311++G(d,p) level. The C7=O1 and C8=O2 bond lengths of the isoindoline fragment are 1.2074(19) Å and 1.2029(19) Å in X-ray structure[29], respectively. These bond lengths were predicted as 1.206 Å for B3LYP. The N1-C7 and N1-C8 bond lengths are 1.4021 (19) Å and 1.4054 (19) Å, respectively, while these bond distances have been computed as 1.415 Å for B3LYP level.

Vibrational spectra

The vibrational band assignments of EPID are illustrated in Table 2. The DFT/B3LYP wavenumbers are in good agreement with experimental observations as seen in Fig. 2. The IR spectra consists of some characteristic bands such as C-H, C=O, C-O, C=C, C-C, CH_2, CH_3 and C-N groups. Generally, C–H ring stretching modes were spread in the region 2900-3150 cm^{-1}[34]. In this EPID molecule, the C-H ring stretching modes were observed at 3062 and 3095 cm^{-1} in the experimental FT-IR spectrum. These modes have been predicted to be at 3063 and 3072 cm^{-1} for B3LYP. The C-H in-plane bending and C-H out-of plane bending modes are found in 1000-1500 cm^{-1} and 600-1000 cm^{-1} region, respectively[26]. The C-H in plane bending modes are observed as mixed modes throughout the region 1094-1517 cm^{-1}. The observed peaks at 715, 791, 818 and 883 cm^{-1} are assigned to C-H out-of plane bending modes, well matched calculated scaled wavenumbers at 699, 769, 810 and 857 cm^{-1}. The CH_3 symmetric and asymmetric methyl stretching bands have been obtained as very weak intensity components at 2932 and 2983 cm^{-1}, respectively. These bands are predicted to be at 2916 and 2988 cm^{-1} for B3LYP, respectively. The CH_2 symmetric stretching mode was observed at 2870 cm^{-1}.

Arjunan *et al*.[21] denoted two carbonyl stretching modes, one appears at 1735 and 1970 cm^{-1} and the other at 1680 and 1750 cm^{-1} for cyclic imides. The C=O stretching vibration varies by conjugation and hydrogen bonding. It also depends on the size of the attached ring. For the 2-chloro-1H-isoindole-1,3(2H)-dione[21], they found the C=O stretching modes at 1726 and 1787 cm^{-1}, and at 1748 and 1790 cm^{-1} for the B3LYP/6-311++G(d,p) level. Similarly, we have predicted the same vibrations at 1718 and 1777 cm^{-1} in the previous work[35]. In the present study, these vibrations are observed at 1715 and 1745 cm^{-1}, are calculated at 1702 and 1753 cm^{-1} for the B3LYP/6-311++G(d,p) level.

The C-O stretching vibration of the ethoxy group is observed as very strong bands at 1046 and 1249 cm^{-1} in FT-IR spectrum and the calculated at 1020 and 1220 cm^{-1}. In 2-(3-chloro-4-(4-chlorophenoxy) phenyl)isoindoline-1,3-dione[35], the C=C and C-C stretching modes are observed in the region 1224-1598 cm^{-1}. In EPID, the C=C and C-C stretching

Table 2 — Comparison of the experimental IR with KBr and calculated vibrational frequencies (cm^{-1})

Assignments [a]	Expt./Calc.
ν (C−H) s R1	3095/3072
ν (C−H) as R3	3062/3063
ν (C−H_3) as	2983/2988
ν (C−H_3) s	2932/2916
ν (C−H_2) s	2870/2878
ν (C=O) s	1745/1753
ν (C=O) as	1715/1702
ν (C=C) R1, R3	1609/1587
ν (C=C) R1	1585/1579
γ(C−H) R3	1517/1482
γ(C−H) R3+α(C−H_2)+α(C−H_3)	1471/1459
γ (C−H) R1	1430/1435
ν (C-N) R2 + ν (C-C) R1	1392/1334
ν (C−O)	1249/1220
ν (C−N) + ν (C−C) R2	1224/1189
γ (C−H) R3	1179/1149
γ (C−H) R3 +ω (C−H_3)	1114/1098
γ (C−H) R3 +ω (C−H_3)	1094/1090
ν (C-O)	1046/1020
ω (C−H_3)	916/899
β (CCC)R1+β(NCO)R2+ω(C−H)R3	883/857
θ(ring) R1, R3	854/831
ω (C−H) R3+δ(C−H_2)+δ(C−H_3)	818/810
ω (C−H) R1 + τ(OCNC)	791/769
ω (C−H) R1 + τ (OCNC)	715/699
β (CCC)R3	632/623
β (CCC) R3 + β (CNC)R2	612/595
β (CCC) R1, R3 +β (COC)	567/553
τ (CCCH) R3	528/511
τ (CCCH) R1	463/446
τ (CCCN) R1, R2	409/405

[a] ν: stretching; α: scissoring; γ: rocking; ω: wagging; δ: twisting; β: bending; τ: torsion; θ: breathing; s: symmetric; as: asymmetric. Abbreviations: R1: C1-C6 ring; R2: C1/C6/C7/N1/C8 ring; R3: C9-C14 ring

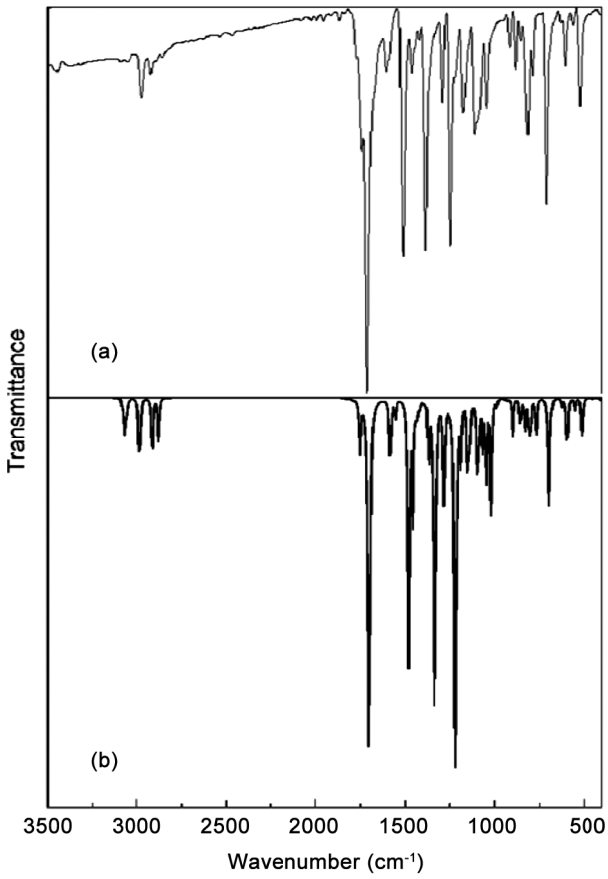

Fig. 2 — (a) Experimental and (b) calculated FT-IR spectra of EPID

vibrations were found in the spectral range 1224-1609 cm^{-1}. The C-N stretching bands have been assigned at 1224 and 1392 cm^{-1} in FT-IR spectrum with medium intensity. The other calculated vibrational frequencies can be seen in Table 2. These values are in agreement with reported values[35,36]. In order to compare the results between the experiment and computation, we present correlation equation based on the calculations. It is described by the following equation:

$$\upsilon_{cal} = 1.00476\ \upsilon_{exp} - 22.26308;\ (R^2 = 0.99971) \quad ...(1)$$

Consequently, the calculated vibrational frequencies are in good consistency with the experimental results.

Electronic absorption spectra

The experimental UV–visible spectrum of EPID recorded with ethanol solvent is shown in Fig. 3. To investigate the excitations in EPID molecule, TD-DFT calculations have been carried out using the B3LYP functional and the 6-311++G(d,p) basis set in gas phase. Besides, TD-DFT calculations were also performed

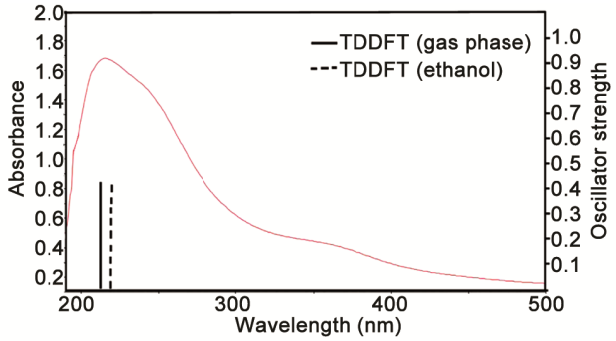

Fig. 3 — UV-visible spectra of EPID in ethanol solvent and the comparison of calculated transitions in gas phase and ethanol solvent with the experimental spectra

Table 3 — Experimental and calculated absorption wavelength, oscillator strengths and energies of title molecule using the TD-DFT method at 6-311++G(d,p) basis set

	λ (nm)	f	E (eV)	[a]Major Contribution ≥ 10%
Experimental	212.3	-	-	-
Gas	211.72	0.426	5.856	H-5→L+1 (10%) H-4→L (10%) H-3→L+1 (58%)
Ethanol	215.18	0.516	5.762	H-4→L+1 (10%) H-3→L (10%) H-2→L+1 (62%)

[a] H: HOMO; L: LUMO

using the IEF-PCM model in ethanol solvent. The predicted maximum absorption wavelength (λ_{max}), oscillator strength (f) and excitation energies (E) along with the majör contribution of transitions are presented in Table 3.

The experimental peak of λ_{max} as determined in ethanol is 212.3 nm, which might be attributed to $\pi \rightarrow \pi*$ transition. The experimental λ_{max} value is in good agreement with the related isoindoline compounds[35,37]. While the theoretical λ_{max} values are calculated to be 211.72 nm in gas phase and 215.18 nm in ethanol solution, which are in very good agreement to its experimental value (see Fig. 3). The frontier molecular orbitals and shown in Fig. 4.

Since neighbouring orbitals may show semi-degenerate energy levels in the boundary region, HOMO and LUMO energy values may not give the description of the frontier orbitals. In order to investigate group contributions to the HOMO and LUMO orbitals, the density of state (DOS) spectrum

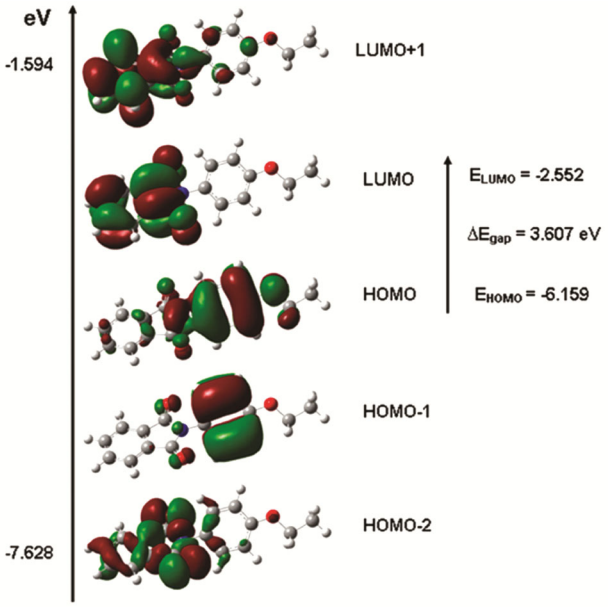

Fig. 4 — Molecular orbital surfaces and energy levels given in parantheses for the HOMO-2, HOMO, LUMO and LUMO+1 of the EPID computed at B3LYP/6-311++G(d,p) level

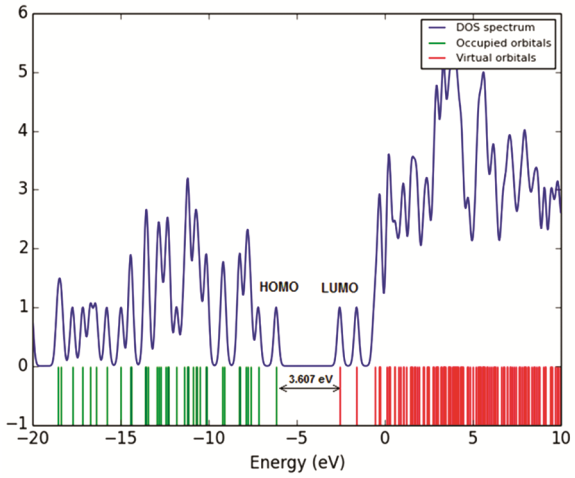

Fig. 5 — Calculated electronic density of states (DOS) for the title compound

was calculated using the Gauss-Sum 2.2 program[38]. DOS spectrA are shown in Fig. 5. While the positive values of the DOS spectrum show a bonding interaction, negative values indicate that there is an anti-bonding interactions. The zero values of DOS show non-bonding interactions[39,40]. The DOS plot showed a simple view of the character of molecular orbitals in a certain energy range.

Chemical reactivity descriptors

The chemical reactivity descriptors of EPID such as chemical hardness (η) and softness (S) were calculated with the DFT/B3LYP method and the 6-311++G(d,p) basis set. Taking into consideration of η, large HOMO–LUMO gap (ΔE_{H-L}) indicates a hard molecule and small ΔE_{H-L} indicates a soft molecule. It is possible to relate the stability of the molecule to η, which indicates that the molecule with least ΔE_{H-L} means it is more reactive and less stable. In this work, the lowering ΔE_{H-L} (3.607 eV) explains the charge transfer interactions that take place within the molecule. The η and S can be measured by means of the HOMO and LUMO energy values for a molecule as: $\eta = (E_L - E_H)/2$ and $S = 1/2\eta$ [34], where E_L and E_H are LUMO and HOMO energies, in order. The measured values of E_L, E_H, η and S for EPID are -2.552 eV, -6.159 eV, 1.804 eV and 0.277 eV, respectively. In comparison with the related isoindoline molecule in the literature, the measured value of η of EPID is smaller than that of 2-(3-chloro-4-(4-chlorophenoxy) phenyl)isoindoline-1,3-dione (η = 1.839 eV) [35]. The results indicate that the EPID molecule is more reactive and less stable than 2-(3-chloro-4-(4-chlorophenoxy) phenyl)isoindoline-1,3-dione[35].

Atomic charge analysis

The atomic charge properties play an important role in vibrational spectra, electronic structure, dipole moment and molecular polarizability. Furthermore, it affects more a lot of properties of molecular systems. The Mulliken atomic charge calculations were performed using the B3LYP/6-311++G(d,p) method. In order to investigate the atomic charge behaviour of EPID in solvent media, we performed DFT calculations in two solvents (ε=78.39, water; ε=24.55, ethanol) at the B3LYP/6-311++G(d,p) level using the IEF-PCM method. Calculated results are listed in Table 4.

In the charge distribution of EPID, C=O bonds in the isoindoline fragment and the carbon atoms bonded with hydrogen atoms carry considerable negative charges, whereas the C1 and C6 atoms have positive charges. The O1 and O2 have larger negative charges than O3 in gas phase. This explains the double bond character of C7=O1 and C8=O2 bonds. On the other hand, the N1 atom of isoindoline ring has positive charge. Depending on the increase of the polarity of the solvent, the atomic charge values of the O1, O2, O3 and N1 atoms increase with the increase of the polarity of the solvent. The plotted atomic charges are shown in Fig. 6.

Molecular electrostatic potential

MEP surface gives a map to understand the charge distributions of the molecule. This map provides

Table 4 — Atomic charges of EPID in gas phase and solution phase

Atom	Gas phase (ε=1)	Ethanol (ε=24.55)	Water (ε=78.36)	Atom	Gas phase (ε=1)	Ethanol (ε=24.55)	Water (ε=78.36)
N1	0.376031	0.817441	0.821883	C14	0.061128	0.250742	0.250002
O1	-0.267007	-0.292229	-0.296224	C15	0.004291	-0.022196	-0.022051
O2	-0.268226	-0.292186	-0.296210	C16	-0.682375	-0.683681	-0.683294
O3	-0.099461	-0.133890	-0.135964	H2	0.198799	0.207593	0.207915
C1	0.799667	0.885224	0.884862	H3	0.179567	0.213075	0.214552
C2	-0.484144	-0.479168	-0.478062	H4	0.180082	0.213075	0.214550
C3	-0.360652	-0.357093	-0.359246	H5	0.197954	0.207594	0.207918
C4	-0.335230	-0.357150	-0.359272	H10	0.210927	0.198388	0.200618
C5	-0.466266	-0.479223	-0.478075	H11	0.196973	0.242857	0.245163
C6	0.622483	0.884900	0.884798	H13	0.198077	0.226084	0.227186
C7	-0.293932	-0.288868	-0.283083	H14	0.196815	0.188406	0.190366
C8	-0.193295	-0.288846	-0.283163	H15A	0.153288	0.172616	0.173496
C9	-0.507803	-1.808933	-1.821709	H15B	0.153725	0.172626	0.173506
C10	0.096593	0.208279	0.206717	H16A	0.146093	0.160866	0.161703
C11	0.470811	0.502376	0.501046	H16B	0.155621	0.157528	0.157478
C12	-0.621897	-0.635336	-0.634408	H16C	0.155826	0.157518	0.157479
C13	-0.174464	0.051607	0.049522				

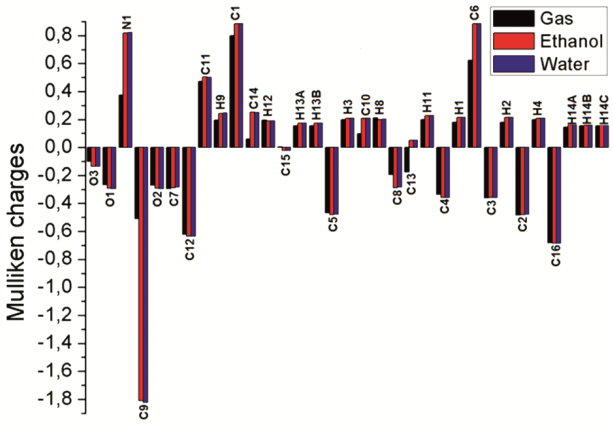

Fig. 6 — Mulliken atomic charges of the EPID

understanding of the hydrogen bonding interactions, nucleophilic reactions and electrophilic attack[41]. As shown in Fig. 7a, the partially positive charge regions (blue) were related to nucleophilic reactivity while partially negative charge regions (red) were related to electrophilic reactivity. The negative MEP values are -0.056 a.u. for O1 atom (deepest red), -0.053 a.u. for O2 atom and -0.036 a.u. for O3 atom and are related to electrophilic reactivity. As seen, an electrophile would preferentially attack the title molecule at O1, O2 and O3 positions. However, extreme positive region is localized on the C4-H4 bond with a value of +0.037 a.u. From these results, the MEP surfaces clearly indicate that the negative charges are concentrated on oxygen atoms, whereas the positive charges are around the hydrogen atoms. Similarly, in the 2D contour maps (Fig. 7b), the greenish-yellow lines are electron deficient region whereas red lines are electron rich (around oxygen). These sites determine how molecules interact with one another and have metallic bonding[42]. These results also support the C-H···O and C-O···π intermolecular interactions in crystal lattice.

NBO analysis

We have executed NBO analysis for investigating electron density (ED) transfer or conjugative interaction in EPID. By using a program which is available in Gaussian 09W, we made NBO calculation. The larger the $E^{(2)}$ value, the more intensive, the interaction between electron donors and electron acceptors[43-45]. The formula of stabilization energy $E^{(2)}$ associated with i(donor)→j(acceptor) delocalization is taken from suitable reference[46,47]. The results of second-order perturbation theory analysis of the Fock Matrix of EPID are summarized in Table 5. Here, the stabilization energies more than 3 kcal mol^{-1} have been listed.

The NBO analysis has unveiled that the intramoleculer interactions formed by the orbital overlap between bonding (C-N), (C-C), (C-O) and (C-H) and anti-bonding (C-N), (C-C), (CO) and (C-H) orbitals results in intramolecular charge transfer giving way to stabilization of EPID. The ED of phenyl ring (~1.88 e) clearly shows strong delocalization. Similarly, the ED of conjugated bond of nine-membered isoindoline fragment (~1.89 e) clearly shows strong delocalization inside the EPID[34].

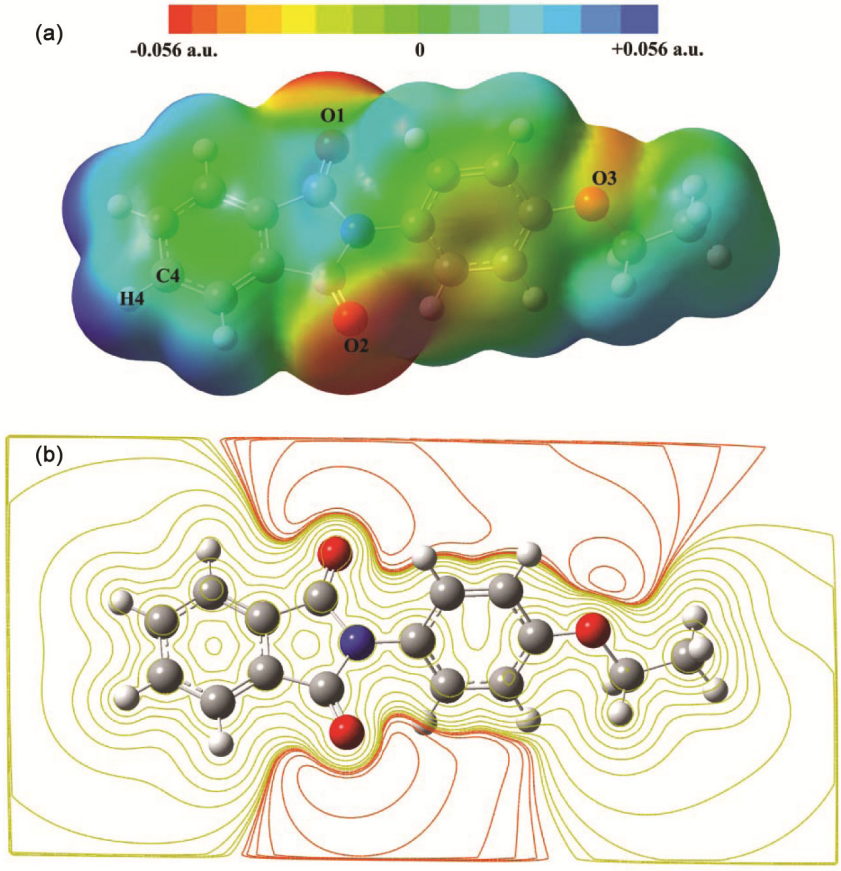

Fig. 7 — (a) Total electron density mapped and (b) the contour maps of electrostatic potential of the EPID

Table 5 — Selected second-order perturbation energies $E^{(2)}$ associated with i→j delocalization

Donor orbital (i)	Type	ED/e	Acceptor orbital (j)	Type	ED/e	$E^{(2)}$ (kcal/mol)[a]	E(j)-E(i) (a.u.)[b]	F(i,j) (a.u.)[c]
N1−C7	σ	1.98251	O2−C8	σ*	0.01037	3.09	1.40	0.059
N1−C8	σ	1.98243	O2−C7	σ*	0.01036	3.08	1.40	0.059
C9−C14	σ	1.97175	C9−C10	σ*	0.02411	4.51	1.28	0.068
C9−C10	σ	1.97229	C9−C14	σ*	0.02472	4.53	1.28	0.068
C9−C10	π	1.68657	C12−C11	π*	0.38930	16.39	0.28	0.062
C9−C10	π	1.68657	C14−C13	π*	0.30930	21.63	0.29	0.071
O2−C8	π	1.97301	C5−C6	π*	0.33801	4.03	0.41	0.039
C7−C1	σ	1.97101	N1−C9	σ*	0.03935	3.97	1.06	0.058
C7−C1	σ	1.97101	C5−C6	σ*	0.02184	4.20	1.24	0.065
C12−C11	σ	1.97784	C12−C13	σ*	0.02259	3.99	1.27	0.064
C12−C11	π	1.65780	C9−C10	π*	0.37339	23.24	0.29	0.074
C12−C11	π	1.65780	C14−C13	π*	0.30930	16.25	0.30	0.062
C12−C13	σ	1.97277	O3−C15	σ*	0.02595	3.01	0.98	0.049
C12−C13	σ	1.97277	C12−C11	σ*	0.02909	3.90	1.26	0.063
C11− H11	σ	1.97641	C9−C10	σ*	0.02411	3.71	1.11	0.057
C11− H11	σ	1.97641	C12−C13	σ*	0.02259	3.92	1.09	0.058
C11−C10	σ	1.97199	O3−C12	σ*	0.02917	4.56	1.07	0.062
C11−C10	σ	1.97199	N1−C9	σ*	0.03935	4.28	1.09	0.061
C11−C10	σ	1.97199	C9−C10	σ*	0.02411	3.24	1.28	0.058
C11−C10	σ	1.97199	C12−C11	σ*	0.02909	3.08	1.26	0.056

(*Contd.*)

Table 5 — Selected second-order perturbation energies $E^{(2)}$ associated with i→j delocalization

Donor orbital (i)	Type	ED/e	Acceptor orbital (j)	Type	ED/e	$E^{(2)}$ (kcal/mol)[a]	E(j)-E(i) (a.u.)[b]	F(i,j) (a.u.)[c]
C1−C6	σ	1.96436	O1−C7	σ*	0.01036	3.31	1.31	0.059
C1−C6	σ	1.96436	O2−C8	σ*	0.01037	3.30	1.31	0.059
C1−C6	σ	1.96436	C1−C2	σ*	0.02184	4.52	1.28	0.068
C1−C6	σ	1.96436	C5−C6	σ*	0.02184	4.52	1.28	0.068
C1−C2	σ	1.97611	C1−C6	σ*	0.02730	5.13	1.30	0.073
C1−C2	π	1.63591	O1−C7	π*	0.23924	17.60	0.28	0.064
C1−C2	π	1.63591	C5−C6	π*	0.33801	21.16	0.29	0.070
C1−C2	π	1.63591	C4−C3	π*	0.31232	19.26	0.28	0.067
C14− H14	σ	1.97753	C9−C10	σ*	0.02411	4.39	1.10	0.062
C14− H14	σ	1.97753	C12−C13	σ*	0.02259	3.65	1.08	0.056
C14−C13	σ	1.97398	O3−C12	σ*	0.02917	3.29	1.07	0.053
C14−C13	σ	1.97398	N1−C9	σ*	0.03935	4.19	1.09	0.061
C14−C13	σ	1.97398	C9−C14	σ*	0.02472	3.17	1.27	0.057
C14−C13	π	1.70347	C9−C10	π*	0.37339	17.73	0.28	0.065
C14−C13	π	1.70347	C12−C11	π*	0.38930	21.89	0.28	0.071
C5− H5	σ	1.97964	C1−C6	σ*	0.02730	4.35	1.11	0.062
C5− H5	σ	1.97964	C4−C3	σ*	0.01554	3.51	1.10	0.055
C5−C4	σ	1.97875	C5−C6	σ*	0.02184	3.17	1.29	0.057
C5−C4	σ	1.97875	C8−C6	σ*	0.07077	4.55	1.13	0.065
C5−C6	σ	1.97611	C1−C6	σ*	0.02730	5.10	1.30	0.073
C5−C6	π	1.63605	O2−C8	π*	0.23981	17.57	0.28	0.064
C5−C6	π	1.63605	C1−C2	π*	0.33778	15.87	0.39	0.071
C5−C6	π	1.63605	C4−C3	π*	0.31232	19.27	0.28	0.067
C10− H10	σ	1.97781	C9−C14	σ*	0.02472	4.45	1.09	0.062
C10− H10	σ	1.97781	C12−C11	σ*	0.02909	3.67	1.08	0.056
C8−C6	σ	1.97097	N1−C9	σ*	0.03935	3.99	1.06	0.058
C8−C6	σ	1.97097	C1−C2	σ*	0.02184	4.20	1.24	0.065
C13− H13	σ	1.97684	C9−C14	σ*	0.02472	3.74	1.08	0.057
C13− H13	σ	1.97684	C12−C11	σ*	0.02909	4.38	1.08	0.061
C4− H4	σ	1.98055	C5−C6	σ*	0.02184	3.31	1.11	0.054
C4− H4	σ	1.98055	C3−C2	σ*	0.01405	3.95	1.09	0.059
C4−C3	π	1.64300	C1−C2	π*	0.33778	14.54	0.39	0.067
C4−C3	π	1.64300	C5−C6	π*	0.33801	19.62	0.29	0.067
C3− H3	σ	1.98055	C1−C2	σ*	0.02184	3.31	1.11	0.054
C3− H3	σ	1.98055	C5−C4	σ*	0.01405	3.96	1.09	0.059
C3−C2	σ	1.97876	C7−C1	σ*	0.07082	4.42	1.16	0.065
C3−C2	σ	1.97876	C1−C2	σ*	0.02184	3.17	1.29	0.057
C2− H2	σ	1.97963	C1−C6	σ*	0.02730	4.35	1.11	0.062
C2− H2	σ	1.97963	C4−C3	σ*	0.01554	3.51	1.10	0.055
C16− H16A	σ	1.98288	O3−C15	σ*	0.02595	3.97	0.79	0.050
C16− H16B	σ	1.98791	C16−H16C	σ*	0.00796	11.80	2.89	0.165
C16− H16C	σ	1.98792	C16−H16C	σ*	0.00796	4.25	2.89	0.099
O3	LP(1)	1.96491	C12−C11	σ*	0.02909	6.84	1.11	0.078
O3	LP(2)	1.84135	C12−C11	π*	0.38930	30.36	0.34	0.096
O3	LP(2)	1.84135	C15−H15A	σ*	0.02598	5.41	0.69	0.057
O3	LP(2)	1.84135	C15−H15B	σ*	0.02598	5.48	0.69	0.057
O1	LP(2)	1.85162	N1−C7	σ*	0.09847	30.33	0.65	0.127
O1	LP(2)	1.85162	C7−C1	σ*	0.07082	18.45	0.72	0.105
N1	LP(1)	1.62644	O1−C7	π*	0.23924	46.94	0.28	0.105
N1	LP(1)	1.62644	C9−C14	σ*	0.02472	3.43	0.84	0.053
N1	LP(1)	1.62644	C9−C10	σ*	0.02411	3.27	0.86	0.052
N1	LP(1)	1.62644	C9−C10	π*	0.37339	11.36	0.30	0.053

(*Contd.*)

Table 5 — Selected second-order perturbation energies $E^{(2)}$ associated with i→j delocalization

Donor orbital (i)	Type	ED/e	Acceptor orbital (j)	Type	ED/e	$E^{(2)}$ (kcal/mol)[a]	E(j)-E(i) (a.u.)[b]	F(i,j) (a.u.)[c]
N1	LP(1)	1.62644	O2−C8	π*	0.23981	47.04	0.28	0.105
O2	LP(2)	1.85167	N1−C8	σ*	0.09852	30.35	0.65	0.127
O2	LP(2)	1.85167	C8−C6	σ*	0.07077	19.21	0.69	0.105
O1−C7	π*	0.23924	C1−C2	π*	0.33778	20.79	0.11	0.080
O2−C8	π*	0.23981	C5−C6	π*	0.33801	169.15	0.01	0.076
C12−C11	π*	0.38930	C14−C13	π*	0.30930	278.49	0.01	0.082
C1−C2	π*	0.33778	C16−H16B	σ*	0.00797	6.15	0.40	0.107
C1−C2	π*	0.33778	C16−H16C	σ*	0.00796	19.04	2.28	0.447
C5−C6	π*	0.33801	C1−C2	π*	0.33778	25.75	0.10	0.078
C4−C3	π*	0.31232	C1−C2	π*	0.33778	26.28	0.11	0.083

[a]$E^{(2)}$,energy of hyper conjugative interactions; [b] Energy difference between donor and acceptor *i* and *j* NBO orbitals; [c]F_{ij} is the Fock matrix element between *i* and *j* NBO orbitals

The measure of delocalization and hyperconjugation is given by $E^{(2)}$ energy. For the studied compound, intramolecular hyperconjugative interactions of π-electrons with the higher energy contributions from C1–C2→O1–C7 (17.60 kcal mol^{-1}), C5-C6 (21.16 kcal mol^{-1}), C4-C3 (19.26 kcal mol^{-1}); C5–C6→O2-C8 (17.57 kcal mol^{-1}), C1-C2 (15.87 kcal mol^{-1}), C4-C3 (19.27 kcal mol^{-1}); C3-C4→C1-C2 (14.54 kcal mol^{-1}), C5-C6 (19.62 kcal mol^{-1}) for the isoindoline ring of the molecule, while C9–C10→C11–C12 (16.39 kcal mol^{-1}), C14-C13 (21.63 kcal mol^{-1}); C11–C12→C9-C10 (23.24 kcal mol^{-1}), C14-C13 (16.25 kcal mol^{-1}); C13–C14→C9-C10 (17.73 kcal mol^{-1}), C11–C12 (21.89 kcal mol^{-1}) for the phenyl ring of the molecule. Hyperconjugative interactions of the σ→σ* transition occurs through weak interaction with 10.25 kcal mol^{-1} energy from various bonds in the compound. The strong interaction, related to the resonance in the compound[34], is electron donating from the $O3_{LP(2)}$, $O1_{LP(2)}$, $N1_{LP(1)}$and $O2_{LP(2)}$ to the antibonding acceptor σ*(N1-C7, C7-C1, N1–C8, C8–C6), and π*(C11–C12, C9–C10) of the skeleton leading to moderate stabilisation energy as shown in Table 5. The $N1_{LP(1)}$ also contributes its electrons to the π* type orbital for O2-C8 and O1-C7. These interactions give the highest stabilisations to the system by 46.94 and 47.04 kcal mol^{-1}, respectively. NBO analysis revealed that, the π*(C11–C12) → π*(C13–C14) interactions give an enormous stabilisation by 278.49 kcal mol^{-1}.

Nonlinear optics

Being applicable in a wide range of areas such as signal processing, data storage technology, laser technology, optical interconnections and optical communications, Nonlinear optics (NLO) study is at the heat of common researches[48]. Calculations of the polarizability (α) and first hyperpolarizability (β) from the Gaussian output have been obtained in detail previously[49], and DFT has been used extensively as an effective method to investigate organic NLO materials[34]. Here, α and β values of the title compound have been calculated at the same basis set. Urea is used frequently as a threshold value for comparative purposes because of one of the prototypical molecules in the study of the NLO properties[50]. The computed values of α and β for EPID are, 31.458 Å^3 and 12.26×10^{-30} cm^5/esu, respectively and are bigger than that of urea (μ=5.042 Å^3 and β=0.78×10^{-30} cm^5/esu). Theoretically, total dipole moment and the first order hyperpolarizability of EPID are greater than that of urea, 6.24 and 15.72 times magnitude of urea, respectively. If it is compared with the similar compound, the value of β of EPID is greater than that of 2-(3-chloro-4-(4-chlorophenoxy)phenyl)isoindoline-1,3-dione (β = 10.45×10^{-30} cm^5/esu)[35]. As a result, this compound is a good candidate as NLO material.

Thermodynamic Properties

The statistical thermodynamic properties of molecules are important for understanding the chemical processes. The thermodynamic functions: entropy (S_m^0), heat capacity ($C_{p,m}^0$) and enthalpy (H_m^0), for the title molecule were obtained from the theoretical harmonic frequencies in the range of temperature 200-700 K and listed in Table 6. For an accurate prediction in determining the thermodynamic functions, we used a scale factor for frequencies (0.96). As can be seen in Table 6, the S_m^0, $C_{p,m}^0$ and

Table 6 — Thermodynamic properties at different temperatures at B3LYP/6-311++G(d,p) level

T (K)	H_m^0 (kcal mol^{-1})	$C_{p,m}^0$ (cal mol^{-1} K^{-1})	S_m^0 (cal mol^{-1} K^{-1})
200	5.678	46.113	112.807
250	8.343	56.564	124.656
298.15	11.408	66.750	135.841
300	11.536	67.138	136.267
350	15.250	77.363	147.698
400	19.459	86.908	158.925
450	24.125	95.614	169.907
500	29.204	103.448	180.603
550	34.655	110.458	190.987
600	40.437	116.723	201.045
650	46.515	122.331	210.773
700	52.859	127.367	220.173

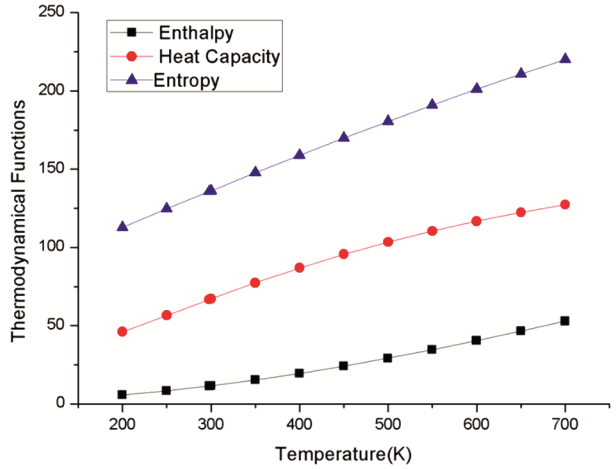

Fig. 8 — Correlation graph of thermodynamical parameters at different temperatures at B3LYP/6-311++G(d,p) level

H_m^0 increase with temperature ranging from 200 to 700 K, as the increase in the molecular vibration intensities show a parallel increase with temperature. The relations between thermodynamic functions and temperatures are shown in Fig. 8. These correlation equations and the corresponding fitting regression factors (R^2) are as follows:

$$C_{p,m}^0 = -7.19694 + 0.29167T - 1.4184\text{x}10^{-4}T^2; (R^2 = 0.99984) \quad ...(2)$$

$$S_m^0 = 61.9624 + 0.26435T - 5.44976\text{x}10^{-5}T^2; (R^2 = 0.99999) \quad ...(3)$$

$$H_m^0 = -2.09756 + 0.02119T - 8.23704\text{x}10^{-5}T^2; (R^2 = 0.99988) \quad ...(4)$$

These thermodynamic data will provide helpful information for further studies of EPID.

Conclusions

2-(4-Ethoxyphenyl)isoindoline-1,3-dione was characterized by experimental FT-IR and UV-visible spectroscopic techniques. Molecular structure and vibrational wavenumbers of 2-(4-ethoxyphenyl) isoindoline-1,3-dione were analyzed using the DFT/B3LYP method with the 6-311++G(d,p) basis set. It is found that the X-ray geometry differs slightly from its optimized counterpart. The vibrational wavenumbers have a good linearity between calculated and experimental results. The TD-DFT calculations are carried out and the calculated results are compared with the experimental absorption spectra. The MEP shows that the electron rich centres are oxygen atoms of 2-(4-ethoxyphenyl) isoindoline-1,3-dione, whereas the proton rich centres are near the hydrogen atoms. The NBO analysis reveals hyperconjugative interaction and stabilization of the molecule. The NBO interacting intensities are relative to the stable energies. The most interacting stable energy is 278.49 kcal/mol^{-1}, $\pi* \rightarrow \pi*$. The calculation of first order hyperpolarizability shows that the title molecule has good NLO properties and it is much greater than that of urea. The HOMO, LUMO orbital energies, $\Delta E_{H\text{-}L}$, chemical hardness, softness, total energy and dipole moment were investigated. These physical parameters are very important for chemical reactivity and biological activities of the title compound. The thermodynamic functions are also obtained and recorded the correlations between the $C_{p,m}^o$, S_m^o, H_m^o and temperatures T.

References

1 Subbarayappa A & Patoliya P. U, *Indian J Chem*, 48B (2009) 545.
2 Belliotti T R, BrinkW A, Kesten S R, Rubin J R, Wustrow D J, Zoski K T, Whetzel S Z, Corbin A E, Pugsley T A, Heffner T G & Wise L D, *Bioorg Med Chem Lett,* 8 (1998) 1499.
3 Sano H, Noguchi T, Tanatani A, Hashimoto Y & Miyachi H, *Bioorg Med Chem,* 13 (2005) 3079.
4 Abdel-Aziz M & Alaa A M, *Eur J Med Chem,* 42 (2007) 612.
5 Alaa A M, ElTahir K E & Asiri Y A, *Eur J Medic Chem,* 46 (2011) 1648.
6 Bhattacharya S. K & Chakrabarti A, *Indian J Exp Biol*, 36 (1998) 118.
7 Medvedev A. E, Clow A, Sandler M & Glover V, *Biochem Pharmacol,* 52 (1996) 385.
8 Chan C. L, Lien E. J & Tokes Z. A, *J Med Chem,* 30 (1987) 509.
9 Alaa A-M, *Eur J Med Chem,* 42 (2007) 614.

10 Sondhi S M, Rani R, Roy P, Agrawal S. K & Saxena A. K, *Bioorg Med Chem Lett,* 19 (2009) 1534.
11 Lima L M, Castro P, Machado A L, Fraga C A M, Lugnier C, de Moraes V L G & Barreiro E J, *Bioorg Med Chem,*10 (2002) 3067.
12 Sridhar S K & Ramesh A, *Biol Pharm Bull,* 24 (2001) 1149.
13 Al-Suwaidan I A, Alanazi A M, El-Azab A S, Al-Obaid A M, ElTahir K E, Maarouf A R, Abu El-Enin M A ,Alaa A M & Abdel-Aziz, *Bioorg Med Chem Lett*, 23 (2013) 2601.
14 Alaa A M, El-Azab A S, Attia S M, Al-Obaid A M, Al-Omar M A & El-Subbagh H I, *Eur J Med Chem*, 46 (2011) 4324.
15 Stryer L, *Biochemistry*, 4th ed, (WH Freeman & Co, New York) 1995.
16 Krysko A A, Chugunov B M, Malovichko O L, Andronati S A, Kabanova T A, Karaseva T L & Kiriyak A V, *Bioorg Med Chem Lett*, 14 (2004) 5533.
17 Masterson L A, Croker S J, Jenkins T C, Howard P W & Thurston D E, *Bioorg Med Chem Lett*, 14 (2004) 901.
18 Kukkola P J, Bilci N A, Ikler T, Savage P, Shetty S S, DelGrande D & Jeng A Y, *Bioorg Med Chem Lett*, 11 (2001) 1737.
19 Fechete I & Jouikov V, *Electrochim Acta,* 53 (2008) 7107.
20 Speck K & Magauer T, *Beilstein J Org Chem*, 9 (2013) 2048.
21 Arjunan V, Saravanan I, Ravindran P & Mohan S, *Spetrochim Acta Part A*,74 (2009) 642.
22 Kolvari E, Ghorbani-Choghamarani A, Salehi P, Shirini F & Zolfigol M A, *J Iran Chem Soc,* 4 (2007) 126.
23 Nicolaou K C & Mathison C J, *Angew Chem Int Ed,* 44 (2005) 5992.
24 Alanazi A M, El-Azab A S, Al-SuwaidanI A, ElTahir K E. H, Asiri Y A, Abdel-Aziz N I & Alaa A M, *Eur J Med Chem,* 92 (2015) 115.
25 Krishnakumar V, Balachandran V & Chithambarathanu T, *Spetrochim Acta Part A,* 62 (2005) 918.
26 Evecen M, Tanak H, Tinmaz F, Dege N & Ilhan I O, *J Mol Struct,* 1126 (2016) 117.
27 Evecen M, Tanak H, Dege N, Kara M, Dogan O E & Agar E, *Mol Cryst Liq Cryst*, 648 (2017) 183.
28 Evecen M, Kara M, Idil O & Tanak H, *J Mol Struct*, 1137 (2017) 206.
29 Duru G, Evecen M, Tanak H & Agar E, *Cryst Rep,* 63 (2018) 1116.
30 Frisch M. J et al. GAUSSIAN 09 (Revision E.01) (Gaussian,Inc.: Wallingford CT) 2009.
31 Dennington II R, Keith T & Millam J, *GaussView, Version 5, Semichem Inc.* (Shawnee Mission, KS) 2009.
32 Casida M E, Jamorski C, Casida K C& Salahub D R, *J Chem Phys,*108 (1998) 4439.
33 Cancès E, Mennucci B & Tomasi J, *J Chem Phys,* 107 (1997) 3032.
34 Tanak H, Koçak F & Agar E, *Mol Phys,*114 (2016) 197.
35 Evecen M, Duru G, Tanak H & Ağar A A, *J Mol Struct,* 1118 (2016) 1.
36 Silverstein R. M, Basseler G. C & Morill C, *Spectroscopic Identification of Organic Compounds,* (Wiley, New York) 1981.
37 Mallesha L, Karthik C. S, Mallu P & Patil V, *SOP Trans Org Chem,* 1 (2014) 21.
38 O'boyle N M, Tenderholt A L & Langner K M, *J Comput Chem,* 29 (2008) 839.
39 Chen M, Waghmare U V, Friend C M & Kaxiras E, *J Chem Phys,* 109 (1998) 6854.
40 Abraham C S, Prasana J C, Muthu S, Rizwana B F & Raja M, *J Mol Struct,* 1160 (2018) 393.
41 Okulik N & Jubert A H, *Internet Electron J Mol Des*, 4 (2005) 17.
42 Tanak H, Agar A A & Büyükgungor O, *J Mol Struct*, 1048 (2013) 41.
43 James C, Raj A A, Reghunathan R, Jayakumar V S & JoeI H, *J Raman Spect*, 37 (2006) 1381.
44 Liu J N, Chen Z R & Yuan S F, *J Zhejiang Univ Sci B,* 6 (2005) 584.
45 Muthu S & Prasath M, *Spectrochim Acta Part A*, 115 (2013) 789.
46 Schwenke D W & Truhlar D G, *J Chem Phys,* 82 (1985) 2418.
47 Gutowski M, van Lenthe J H & van Duijneveldt F B, *J Chem Phys,* 98 (1993) 4728.
48 Yu Z, Sun G, Liu Z, Yu C, Huang C & Sun Y, *J Mol Struct,* 1030 (2012) 113.
49 Thanthiriwatte K S & De Silva K N, *J Mol Struct,* 617 (2002) 169.
50 Al-Abdullah E S, Mary Y S, Panicker C Y, El-Brollosy N R, El-Emam A A, van Alsenoy C & Al-Saadi A A, *Spectrochim Acta Part A,* 133 (2014) 639.